Transactions on Ecology and the Environment vol 7, © 1995 WIT Press, www.witpress.com, ISSN 1743-3541

Finite volume methods for two-dimensional groundwater pollutant transport

A. Balaguer[a], C. Conde[b], A. Hidalgo[b], J.A. López[a], V. Martínez[a]
[a]*Universitat Jaume I, Departament de Matemàtiques, Campus Penyeta Roja, 12071 Castellón, Spain*
[b]*Univ. Politécnica de Madrid, ETSI Minas, Dep. de Matemática Aplicada y Métodos Informáticos, C/. Rios Rosas, 21, 28003 Madrid, Spain*

Abstract.

A modelling procedure of the two-dimensional advection-dispersion equation based on a finite volume method for the spatial discretization is presented in this paper. Control volumes are made up over a standard triangulation, which give the grid nodes where we obtain the numerical solutions. A first order accurate interpolation is used over each triangle that contains the control volume. Some idealized initial value problems are studied showing the practical advantages and disadvantages of the method in comparison with analytical solutions.

1 Introduction.

The advection-dispersion equation is used extensively in studying and analyzing the transport of contaminants through groundwater systems. A variety of improved numerical methods has been presented in recent years to deal with numerical difficulties (spurious oscillations, numerical diffusion, peak damping, phase lag..) arising in the solution of advection-dominated transport problems

The use of upwinding methods has been a very popular remedy in both finite difference schemes and finite element methods (see Ikeda [2]). However while tradicional upwinding methods work well for steady state problems, they lead to over-diffusive solutions for time dependent problems (see Balaguer et al. [1]).

The objective of the present paper is to introduce two finite volume schemes for solving the two dimensional advection-dispersion equation based on a centered numerical scheme and a first order interpolation. Their behaviour is analyzed in two simple two-dimensional problems with several transport types.

2 General formulation.

The new numerical scheme is developed to compute the physically relevant solution of the initial-boundary value problem associated with the two-dimensional advection-dispersion equation:

$$\frac{\partial u}{\partial t} + \vec{\nabla}\cdot(\vec{v}\cdot u) - \vec{\nabla}\cdot\left(\mathbf{K}\cdot\vec{\nabla}u\right) = f(x,y,t) \quad \text{in } \Omega\times]0,T[\quad (1)$$

$$u(x,y,0) = c_0(x,y) \quad \text{in } \Omega \quad (2)$$

$$u(x,y,t) = c^D(x,y,t) \quad \text{in } \delta\Omega_1\times]0,T[\quad (3)$$

$$\mathbf{K}\frac{\partial u}{\partial \vec{n}} = 0 \quad \text{in } \delta\Omega_2\times]0,T[\quad (4)$$

where $u(x,y,t)$ is the only one unknown function and represent the concentration of pollutants at a time t in a spatial domain $\Omega \subset \mathcal{R}^2$, $\vec{n}$ is the outward unit normal on $\delta\Omega$, $\delta\Omega = \delta\Omega_1 \cup \delta\Omega_2$ is the boundary of Ω, $\vec{v}(x,y,t)$ is the vector pore velocity, $\mathbf{K}(x,y,t)$ is a mathematical representation of the dispersion tensor:

$$\mathbf{K} = \begin{pmatrix} K_{11} & K_{12} \\ K_{21} & K_{22} \end{pmatrix}$$

$\vec{\nabla} = \left(\frac{\partial}{\partial x}, \frac{\partial}{\partial y}\right)$, f take up the fluxes balance over Ω and c_0, c^D are known and yielded by the initial and Dirichlet boundary conditions respectively.

We assume that Ω is a polygonal, bounded domain of $\mathcal{R}^2$ that can be discretized by a standard triangulation T_h. For every vertex $\mathbf{x}_i$ of each triangle, which is a node of the numerical methods, we define a control volume as the union of the subtriangles which result on dividing every triangle having x_i as a vertex by using the median lines (figure I).

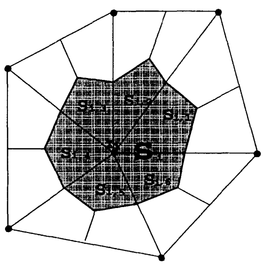

Figure I. Control volumes in a general triangulation.

The space discrete equations are obtained by integrating the governing equation over each control volume and approximating the integrals by standard numerical integration rules. If we denote by S_i the control volume associate to node $\mathbf{x}_i$ we obtain the next:

$$\int_{S_i} \frac{\partial u}{\partial t} \, d\Omega + \int_{\delta S_i} (\vec{\mu_i} \cdot \vec{v}) \cdot u \, d(\delta\Omega) - \int_{\delta S_i} (\vec{\mu_i} \cdot \mathbf{K}) \cdot \vec{\nabla} u \, d(\delta\Omega) = 0$$
$$\forall i = 1, \ldots N \quad \forall t \in]0, T[$$

where the Green's formula has been employed to transform the second and third integrals on the left-hand side to integrals over the cell boundary δS_i, $\vec{\mu_i}(x, y)$ is the outward unit normal on δS_i and N is the vertex number of T_h at which we do not consider a Dirichlet boundary condition. Integration in control volumes associated to vertex $\mathbf{x}_i = (x_i, y_i)$ inclosed in $\delta\Omega_1$ is omited and their resultant equations are replaced by $u^{n+1}(x_i, y_i) = c^D(x_i, y_i, t^{n+1})$.

Time integration is obtained by choosing t^n $n = 0, \ldots, NT$ time discrete values with $t^0 = 0$ and $t^{NT} = T$, and by using a Crank Nicholson scheme so:

$$\int_{S_i} u^{n+1} \, d\Omega + \frac{1}{2} \triangle t_n \, \Delta_i^{n+1} = \int_{S_i} u^n \, d\Omega - \frac{1}{2} \triangle t_n \, \Delta_i^n \qquad (5)$$
$$\forall i = 1, \ldots, N \qquad n = 0, \ldots, NT - 1$$

being $\triangle t_n = t^{n+1} - t^n$ and

$$\Delta_i^n = \int_{\delta S_i} (\vec{\mu_i} \cdot \vec{v}^n) \cdot u^n \, d(\delta\Omega) - \int_{\delta S_i} (\vec{\mu_i} \cdot \mathbf{K}^n) \cdot \vec{\nabla} u^n \, d(\delta\Omega) \qquad (6)$$

The superindex "n" denotes the function values at t^n. Notice that this time scheme is second order accurate.

3 Approximations to space integrals.

Now we are going to define the numerical evaluation of the integrals in (5) and (6). S_i can be expressed as the union of several subdomains (see figure 1): $S_i = S_{i,1} \cup S_{i,2} \cup \ldots \cup S_{i,Ni}$ being "Ni" the number of triangles containing to the vertex "$\mathbf{x}_i$" (which has associated the finite volume S_i). Such triangles are denoted by $T_{i,j}$ $\forall j$. Thus $S_{i,j} = S_i \cap T_{i,j}$ $\forall j$. In each $T_{i,j}$ we approximate u^n by means of a polynomial of degree equal to 1:

$$u^n(x, y) \approx a_{ij,0}^n + a_{ij,1}^n \cdot x + a_{ij,2}^n \cdot y = P_{i,j}^n(x, y) \quad \forall (x, y) \in T_{i,j} \qquad (7)$$

To evaluate the integral of the diffusive term ($\delta\overline{S}_{i,j} = \delta S_{i,j} \cap int(\Omega)$):

$$\int_{\delta S_i} (\vec{\mu_i} \cdot \mathbf{K}^n) \cdot \vec{\nabla} u^n \, d(\delta\Omega) = \sum_{j=1}^{Ni} \left(\int_{\delta\overline{S}_{i,j} \cap \delta S_i} (\vec{\mu_i} \cdot \mathbf{K}^n) \cdot \vec{\nabla} u^n \, d(\delta\Omega) + \int_{\delta S_{i,j} \cap \delta\Omega} (\vec{n} \cdot \mathbf{K}^n) \cdot \vec{\nabla} u^n \, d(\delta\Omega) \right)$$

we need evaluate the value of the concentration gradient $\vec{\nabla} u^n$ along each $\delta\overline{S}_{i,j} \cap \delta S_i$. The approximation in $\delta S_{i,j} \cap \delta\Omega$ may be omited because of (4) so we consider a Neumann boundary condition in a cell where we do not consider a Dirichlet boundary condition. Because u^n is given in each $T_{i,j}$ by a P1 interpolation (after (7)) we consider that $\vec{\nabla} u^n$ is constant into $T_{i,j}$ and therefore we approximate ($\vec{\mu}_i = (\vec{\mu}_{i,1}, \vec{\mu}_{i,2})$):

$$\int_{\delta \overline{S}_{i,j} \cap \delta S_i} (\vec{\mu}_i \cdot \mathbf{K}^n) \cdot \vec{\nabla} u^n \; d(\delta\Omega) \;\approx\; \frac{\partial P^n_{i,j}}{\partial x} \int_{\delta \overline{S}_{i,j} \cap \delta S_i} (\vec{\mu}_{i,1} \cdot K_{11} + \vec{\mu}_{i,2} \cdot K_{21}) \; d(\delta\Omega) + \frac{\partial P^n_{i,j}}{\partial y} \int_{\delta \overline{S}_{i,j} \cap \delta S_i} (\vec{\mu}_{i,1} \cdot K_{12} + \vec{\mu}_{i,2} \cdot K_{22}) \; d(\delta\Omega)$$

In order to approximate the convective term we also consider the integrals in the subdomains boundary:

$$\int_{\delta S_i} (\vec{\mu}_i \cdot \vec{v}^n) \cdot u^n \; d(\delta\Omega) \;=\; \sum_{j=1}^{Ni} \int_{\delta S_{i,j} \cap S_i} (\vec{\mu}_i \cdot \vec{v}^n) \cdot u^n \; d(\delta\Omega)$$

However now $\delta S_{i,j} \cap S_i$ is splitted into bisegments $\delta S^1_{i,j}$ and $\delta S^2_{i,j}$ joining the centroid of $T_{i,j}$ to the middle of the segments $[\mathbf{x}_i, \mathbf{x}_j]$ and $[\mathbf{x}_i, \mathbf{x}_k]$ respectively being $\mathbf{x}_j$ and $\mathbf{x}_k$ the vertex of $T_{i,j}$ different from $\mathbf{x}_i$ (figure II.). so:

$$\int_{\delta S_{i,j} \cap S_i} (\vec{\mu}_i \cdot \vec{v}^n) \cdot u^n) \; d(\delta\Omega) \;=\; \int_{\delta S^1_{i,j}} (\vec{\mu}_i \cdot \vec{v}^n) \cdot u^n \; d(\delta\Omega) + \int_{\delta S^2_{i,j}} (\vec{\mu}_i \cdot \vec{v}^n) \cdot u^n \; d(\delta\Omega) \;+\; \int_{\delta S_{i,j} \cap \delta\Omega} (\vec{\mu}_i \cdot \vec{v}^n) \cdot u^n \; d(\delta\Omega) \tag{8}$$

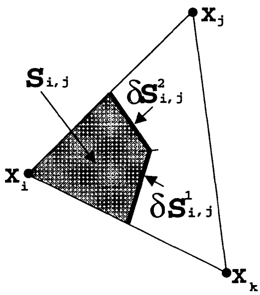

Figure II. An example of $\delta S^1_{i,j}$ and $\delta S^2_{i,j}$.

Notice that $\vec{\mu}_i(x,y) = \vec{\mu}^k_{ij} = constant \; \forall (x,y) \in \delta S^k_{i,j} \; k = 1,2$ and $\vec{\mu}_i(x,y) = \vec{\mu}^3_{ij} = constant \; \forall (x,y) \in \delta S_{i,j} \cap \delta\Omega$. Thus we approximate the above integrals in (8) by a gaussian quadrature ($\delta S^3_{i,j} = \delta S_{i,j} \cap \delta\Omega$):

$$\int_{\delta S^k_{i,j}} (\vec{\mu}_i \cdot \vec{v}^n) \cdot u^n \; d\delta\Omega \;\approx\; \sum_{l=1}^{IPNB} \gamma_l \cdot \left(\vec{\mu}^k_{ij} \cdot \vec{v}^n(\alpha_l, \beta_l)\right) \cdot u^n(\alpha_l, \beta_l)$$

being $IPNB$ the number of integration nodes, γ_l the coefficients of the numerical quadrature and (α_l, β_l) the coordinates of the integration nodes.

Because we have assumed a P1 interpolation in each triangle we may use the midpoint rule with $IPNB = 1$. Moreover numerical experiments have shown that there are not a lot of variation in solutions when we utilize a gaussian quadrature of a higher order.

Integration over the whole control volume is also approximated in each $S_{i,j}$ by a gaussian quadrature based on a only one integration node:

$$\int_{S_i} u^n \, d\Omega = \sum_{j=1}^{Ni} \left(\int_{S_{i,j}} u^n \, d\Omega \right) \approx \sum_{j=1}^{Ni} \left(\text{Area}(S_{i,j}) \cdot u^n(\psi_{i,j}, \eta_{i,j}) \right) \qquad (9)$$

being $(\psi_{i,j}, \eta_{i,j})$ the midpoint of $S_{i,j}$. Numerical solutions obtained with this integration formula will be compared in the following section with the ones obtained with a numerical quadrature over the whole control volume:

$$\int_{S_i} u^n \, d\Omega \;=\; \text{Area}(S_i) \cdot u^n(x_i, y_i) \qquad (10)$$

where $\mathbf{x}_i = (x_i, y_i)$ is the node that has associated the control volume S_i.

4 Numerical examples.

In this section we present some results of the finite volume methods derived in the above section. Testing and verification of their behaviour are performed in two basically initial value problems at which we assume a steady flow field, horizontal along the x axis (i.e. $\vec{v}(x,y) = (v_x, 0) = constant\ \forall(x,y) \in \Omega$), a diagonal dispersion tensor (i.e. $K_{12} = K_{21} = 0$) and $f(x,y,t) = 0$. The initial condition is based on a Gaussina hill, which may be expressed by the next form:

$$c_{T^{in}}(x,y) \;=\; \frac{1}{4 \cdot \pi \cdot T^{in} \cdot \sqrt{K_{11} \cdot K_{22}}} \exp\left(-\frac{(x - v_x \cdot T^{in})^2}{4 \cdot K_{11} \cdot T^{in}} - \frac{y^2}{4 \cdot K_{22} \cdot T^{in}} \right)$$
$$0 < T^{in} < T$$

Neumann boundary conditions are assumed in the whole $\delta\Omega$ so $\delta\Omega_2 = \delta\Omega$. The analytical solution is known and it is given by $u(x,y,t) = u_{T^{in}+t}(x,y)$.

Problem 1 concerns the solution of the only one diffusive transport $(v_x = 0)$ of a initial concentration hill with $T^{in} = 10$ hours and with $K_{11} = K_{22} = 0.03\ \text{m}^2./\text{h}.$. Numerical results obtained with each one of integration formulas (10) and (9) and their comparison with the analytical solution after $t = 10$ hours of simulation are presented in figure 1. Numerical simulation obtained with a spatial discretization based on a triangulation as the one of figure III a. with $\triangle x = \triangle y = \frac{1}{2}$ and $\triangle t_n = \frac{1}{2}\ \forall n$, shows a peak clipping so the peak of the analytical solution has a smaller value than the one obtained by using (10) approximation and a higher value than the one obtained with (9). Otherwise, if we choose some smaller values of $\triangle x = \triangle y = \triangle t_n$ (for example $\frac{1}{4}$), numerical solutions are very accurate to analytical solution.

Transactions on Ecology and the Environment vol 7, © 1995 WIT Press, www.witpress.com, ISSN 1743-3541

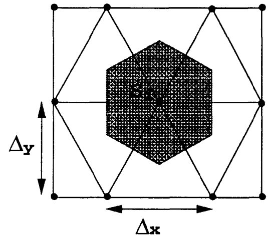

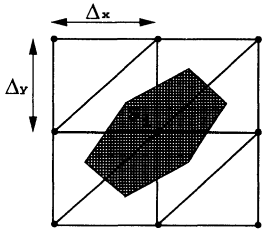

figure III. Two mesh used in numerical examples.

Problem 2 consider a horizontal steady flow with magnitude $v_x = 1$ m./h. and assumes an initial gaussian hill with $T^{in} = 2$, $c_2(x,t)$. Diffusive transport is given again by the following parameters $K_{11} = K_{22} = 0.03$. Figure 2 depicts the concentration profiles after 10 hours of simulation as obtained with the (10) and (9) approximations, using a triangulation based on mesh IIIa.. It is seen that both approximations give solutions with numerical oscillations and the numerical peak is displaced a little on the left. Both errors are more importants when we use the approximation (10). During a time interval $\triangle t_n$, the distribution of concentration at grid points is not transported to other grid points and this introduce a less peak concentration. Because we use mass conservative schemes, the lost peak mass is compensated by overspreading this lost mass to some grid points and self-correcting the overspreading at some other grid points such that the net integrated mass under the distribution curve at time t^{n+1} is the same as that at t^n. This creates spurious oscillations. Moreover the behaviour of numerical schemes is the same when we use the mesh IIIb) for defining the grid nodes.

Concentration profiles obtained with mesh IIIb) along the center of the plume in the trasverse direction are compared with the analytical solution in figure 3. Numerical solution resulting from the approximation (9) shows a more good agreement with the analytical than the one resulting from the (10) approximation, even though we use a finer mesh.

Numerical errors can be avoided in both schemes by using some smaller values of $\triangle x = \triangle y$ so the Peclet number in the x direction $Pe_x = \frac{v_x \cdot \triangle x}{K_{11}}$ satisfies $Pe_x \leq 3$. We may see this in figure 4. in a example where physical diffusion is higher ($K_{11} = K_{22} = 0.1$).

5 Summary and conclusions.

Several finite volume methods have been presented in this paper based on a first order spatial interpolation of the concentration over each triangle of a standard triangulation. Two test problems have been used to demostrate the behaviour of two different integration techniques over the control volumes: the first one is a cuadrature formula over the whole control volume (given in (10)) and the second one is a gaussian cuadrature over each subdomain resulting of the intersection between the control volume S_i and each triangle that has the node $\mathbf{x}_i$ as a vertex (it is given in (9)).

We may conclude that both finite volume methods are clearly limited in their ability to resolve sudden jumps in value within a small number of grid points. Numerical solutions show then spurious oscillations and/or peak clipping, more importants with the approximation (10). Numerical errors can be avoided by using the approximation (9) defining a finer mesh so for the general problem the Peclet number defined in the above section has a value smaller o equal to 3.

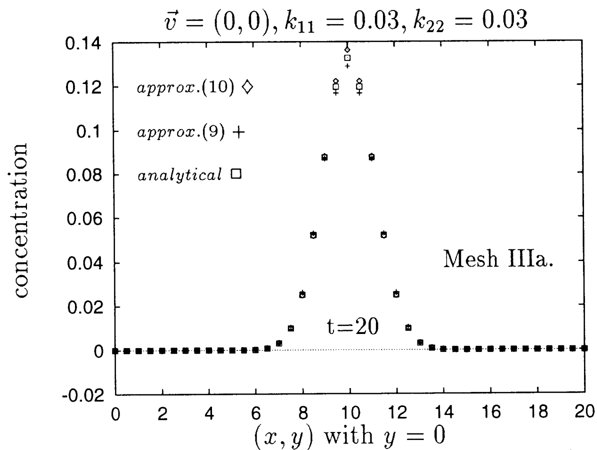

figure 1. Problem 1 with $\triangle x = \triangle y = \triangle t_n = \frac{1}{2}$

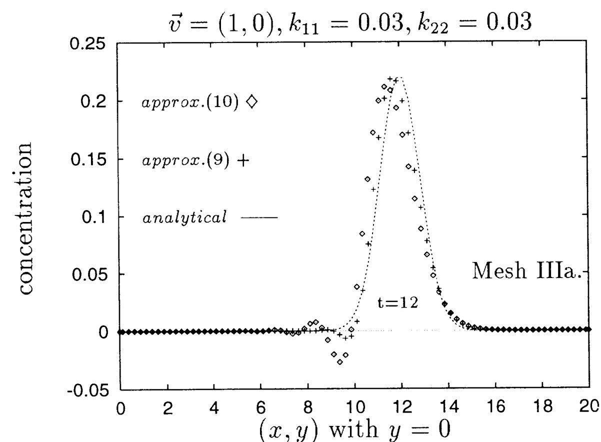

figure 2. Problem 2 with $\triangle x = \triangle y = \triangle t_n = \frac{1}{4}$

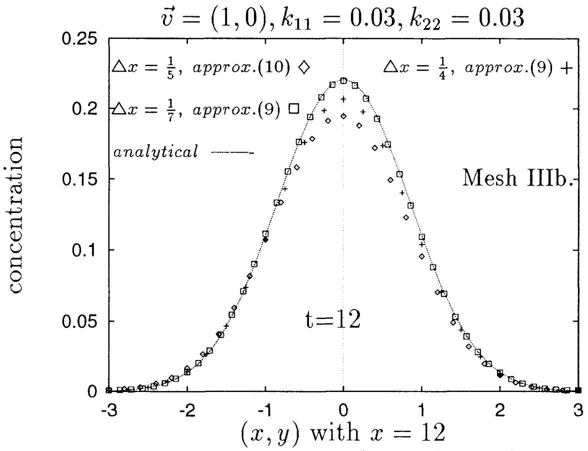

figure 3. Problem 2 with $\triangle x = \triangle y = \triangle t_n$

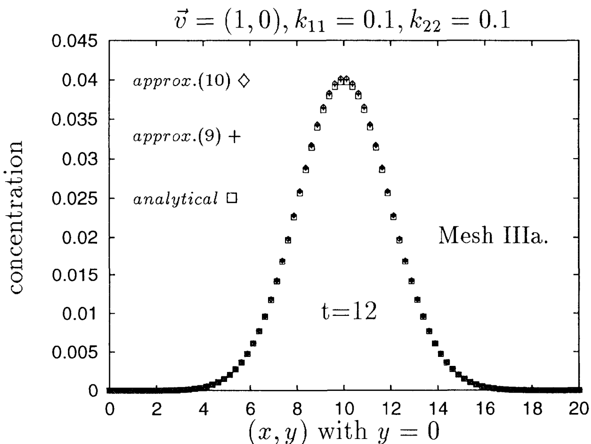

figure 4. Problem 2 with $\triangle x = \triangle y = \triangle t_n = \frac{1}{4}$

Ackonowledgements.
Angel Balaguer acknowledges the Consellería de Cultura, Educació i Ciencia of the Generalitat Valenciana for a fellowship. The work of Carlos Conde has been partially supported by ENRESA, Spanish nuclear waste disposal company, under contract number 0700442.

References

[1] Balaguer A., Conde C., López J.A., Martínez V. *Un modelo numérico bidimensional de transporte de resíduos radiactivos.* Proceedings of XX reunión anual SNE. Córdoba, Spain, 1994 (in press).
[2] Ikeda T. *Maximum principle in finite element models for convection-diffusion phenomena.* North-Holland, New York, 1983 (pp 158)